https://doi.org/10.20965/jrm.2023.p0510

Paper:

Investigation of Obstacle Prediction Network for Improving Home-Care Robot Navigation Performance

Mohamad Yani[*,**], **Azhar Aulia Saputra**[**], **Wei Hong Chin**[**], **and Naoyuki Kubota**[**]

[*]Department of Computer Engineering, Faculty of Electronics and Intelligent Industry Technology, Institut Teknologi Telkom Surabaya
Surabaya 60231, Indonesia
E-mail: mai@ittelkom-sby.ac.id

[**]Department of Mechanical System Engineering, Faculty of System Design, Tokyo Metropolitan University
6-6 Asahigaoka, Hino, Tokyo 191-0065, Japan
E-mail: {mohamad_yani@ed., aa.saputra@, weihong@, kubota@}tmu.ac.jp

[Received February 2, 2022; accepted February 9, 2023]

Home-care manipulation robot requires exploring and performing the navigation task safely to reach the grasping target and ensure human safety in the home environment. An indoor home environment has complex obstacles such as chairs, tables, and sports equipment, which make it difficult for robots that rely on 2D laser rangefinders to detect. On the other hand, the conventional approaches overcome the problem by using 3D LiDAR, RGB-D camera, or fusing sensor data. The convolutional neural network has shown promising results in dealing with unseen obstacles in navigation by predicting the unseen obstacle from 2D grid maps to perform collision avoidance using 2D laser rangefinders only. Thus, this paper investigated the predicted grid map from the obstacle prediction network result for improving indoor navigation performance using only 2D LiDAR measurement. This work was evaluated by combining the configuration of the various local planners, type of static obstacles, raw map, and predicted map. Our investigation demonstrated that using the predicted grid map enabled all the local planners to achieve a better collision-free path by using the 2D laser rangefinders only rather than the RGB-D camera with 2D laser rangefinders with a raw map. This advanced investigation considers that the predicted map is potentially helpful for future work in the learning-based local navigation system.

Keywords: safety, unseen obstacle, obstacle prediction networks

1. Introduction

Home-care robots are frequently operated in designed environments for and occupied by humans. Especially in countries with low birthrate issues, such as Japan and many other developed countries, home-care manipulation robots such as Toyota HSR are possible solutions to improve the quality of life (QOL) for aged people in the home environment or the public area [1]. These environments usually consist of various complex objects such as chairs, tables, and sports equipment with a narrow workspace. At the same time, we expect to increase the robot's adaptability in various environments and ensure the user's safety and comfort.

The home-care manipulation robot generally can be combined with the manipulation and navigation task as whole-body manipulation or decomposed for different purposes and needs [2–5]. The decomposed task of the home-care manipulation robot is typically defined by a set of mobile base navigation and arm manipulation subgoals. Thus, navigation significantly enhances the arm manipulation tasks, such as picking, placing, pulling, and pushing. Particularly, Toyota HSR has a shorter arm [1] and less degree of freedom (DoF) than other domestic home-care manipulation robots such as Fetch [6], Tiago [a], and PR2 [7]. Moreover, the compact body of HSR is more suitable for navigating narrow and small environments such as a house, office, and hospital room. These abilities have been shown in [1, 2, 6–8], and the result shows that HSR always performs the base navigation task to reach the grasping object.

Toyota HSR has several sensors, such as 2D laser rangefinders to build the 2D map and sense the obstacle for navigation, IMU for localization, and several cameras, including an RGB-D camera and a pair of RGB cameras in a stereo setup in the head part. However, the possibility of low real-time performance is expected if we simultaneously apply several fusion perception modules for navigation and manipulation. It is due to the computational process of a large amount of labeled data from object recognition and 3D map reconstruction. On the other hand, it is difficult for a home-care robot to detect the surrounding approaching dynamic obstacle, such as a walking human toward the robot position where the walking direction is out of camera view as shown in **Fig. 1** description. Thus, the robot requires a more extensive range of sensors such as 2D laser rangefinders to generate a safer path from laser rangefinders and information occupancy of obstacles from a 2D map.

Nevertheless, horizontal laser rangefinders only scan

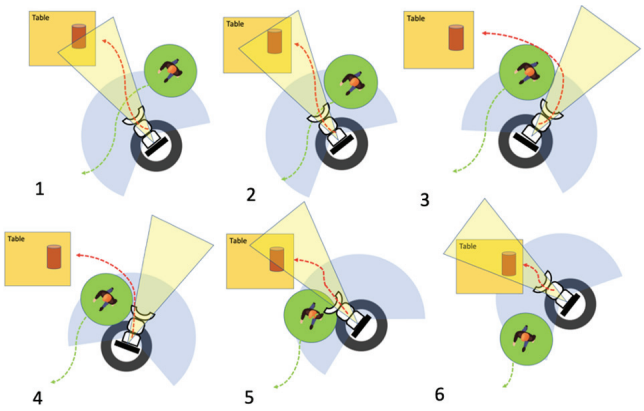

Fig. 1. The human walking direction toward robot position is out of robot camera view. The robot changes the trajectory because the human walking is detected by 2D LiDAR.

one slice of the environment and, as a result, most often miss the big part of obstacles. Consequently, the resulting 2D occupancy maps frequently may not accurately represent the occupied area in the environment. For instance, when the laser rangefinders detect the table and chairs, the scanning result only shows the table and chair legs in a 2D occupancy map. Therefore, it may produce the wrong trajectory planning from global and local planners when the mobile manipulation robot performs the navigation task. **Fig. 2** described the unseen obstacle or partially observed object examples viewed by laser rangefinders in the home environment that we obtained from Toyota HSR ROS package [b] for SH and from AWS RoboMaker [c] for LH. Many previous works [9–13, d] have proposed DRL-based local planners and used the recorded 2D maps from laser rangefinders to train the deep neural networks with static obstacles and reactive human walking. This trial-and-error strategy lets the robot learn static and dynamic obstacle avoidance behavior based purely on observations. The training process is accelerated with deep neural networks, and recent research showed excellent results in robot navigation. The purpose of using 2D LiDAR only in these navigation approaches is to reduce the computational cost during learning navigation and avoid active walking humans with simple static obstacles in indoor environments. However, the unseen obstacles or partially observed objects are not considered as the navigation task problem in these recent works [9–13, d].

Based on this report [14], the tiny or incomplete obstacle representation in a 2D occupancy map can trap the robot when attempting to avoid the collision. Moreover, the recent result from [14] has shown an outstanding solution to solve the unseen obstacle problem in several indoor environments without inflation layer or safety layer parameter tuning using the feature of ROS navigation stack. Since all the local planners depend on the 2D occupancy map information to find the collision-free path, combining the ROS navigation stack with this work [14] is essential to perform obstacle avoidance more efficiently using 2D LiDAR only. However, to apply and utilize this method in different types of robots such as Toyota HSR, we should conduct further investigation and evaluation to measure the effectiveness and limitation with different kind of obstacles and existing global and local planners.

We make the following contributions:

- We present an investigation and comparison study for possible solutions to the unseen obstacle problem in the home-care robot (Toyota HSR) navigation.
- We compare obstacle prediction network results with a raw map and sensor fusion (obstacle data acquired through the combination of the RGB-D camera and 2D LiDAR) and various conventional local planners in simulated environments to find its methods' upper limit and efficiency.

Since the DRL local planner uses the recorded map to avoid static obstacles, this investigation can be considered as a future work application on the learning-based local planner.

The paper is arranged as follows. Section 2 explains the related work of the investigation method. Section 3 describes the proposed integration navigation system's obstacle prediction network results. Section 4 explains the experimental setup and defined parameters that we used in the evaluation. Section 5 shows the evaluation result and discussion. Finally, conclusions and future work suggestions are presented in Section 6.

2. Related Work

Mobile manipulation robot tasks are typically specified by end-effector and base navigation subgoals. Hence, navigation has the main contribution to the mobile manipulation tasks, such as reaching and placing the target object. According to [12, 15], typical ROS navigation approaches consist of a combination of global and local planners approaches. Global planner approaches, such as potential field strategies, cell decomposition, roadmaps, and Dijkstra, commonly require a comprehensive model of the environment. The advantage of the global approach is that it can compute a complete trajectory from the initial position to the desired position. Regardless, these approaches are inadequate to generate reactive avoidance behavior in the robot's local vicinity. Integrating with the local planners approaches [16] can improve the navigation performance in this case.

The classical local planners that are usually used in the ROS-based navigation system are the trajectory rollout or base local planner [e] and the dynamic window approach (DWA) [16]. They are planners that provide control for a mobile robot on a 2D occupancy map space. Using a 2D occupancy map, the local planners calculate the path for a mobile robot to move from the initial position to the desired position. The DWA approach differs from the trajectory rollout approach in controlling discretized space. While the trajectory rollout checks all the next states in simulation [e], the DWA local planner checks only the collision-free area directly after the current state.

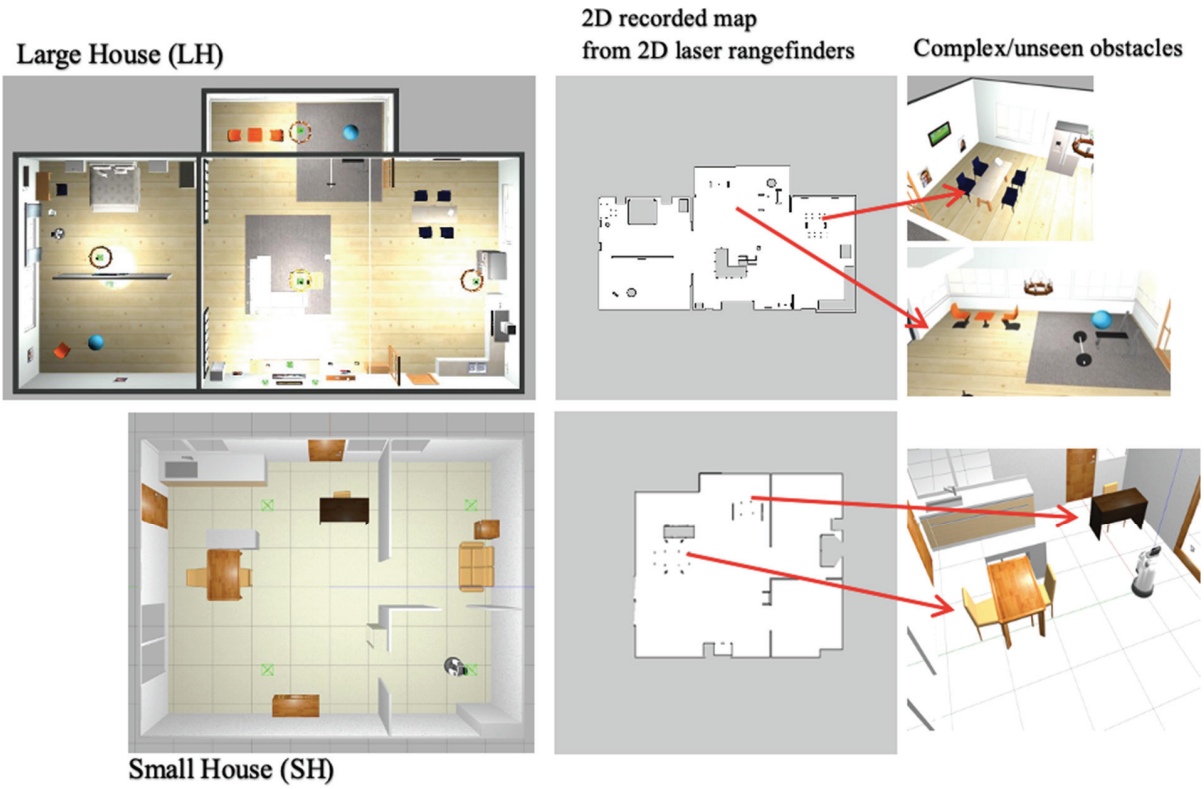

Fig. 2. Simulated home environment. The left part is the realistic simulated environment; the center part indicates the 2D recorded map obtained from laser observation; the right part shows the details of the complex obstacle that 2D laser rangefinders cannot fully detect.

Other traditional local planners are the elastic band (EBand) [17] and the timed elastic band (TEB) [18]. The EBand planner uses the bubble area to specify a subset of the maximum location for a free space in a particular configuration. It enables the robot to travel in all directions without colliding [17]. The bubble is formulated using the simplified model of the robot in conjunction with information available on the 2D occupancy map. The bubble band considers forces from obstacles and internal forces trying to minimize the force between neighboring bubbles. The EBand is a planner that produces a collision-free and deformable trajectory. It deforms the computed path in real-time to keep it away from obstacles and continues to deform as obstacles update. This enables the mobile robot to adjust to a suddenly moving object. TEB operates on the same concept as EBand. However, it minimizes the time cost function rather than applying energy optimization [18].

With the current achievements of deep learning and reinforcement learning, indoor learning-based robot navigation has also gained much attention in recent years [9,11,19–21, d]. In the work of Guldenring et al. [9], their learning-based local planner could avoid the active human walking and static obstacles such as walls and corridors based on the 2D recorded occupancy maps and using 2D LiDAR sensor only by utilizing the simulated 2D human walking (PedSim [f]) and ROS navigation stack plugins. However, the 2D LiDAR only detects one slice of the environment and often misses the big parts of objects. Thus, the resulting 2D occupancy maps usually do not accurately represent the free area in the robot workspace. Based on these works [9, 12, 13], the particular obstacles should be chosen and prepared beforehand based on the robot's ability and sensor limitation. Another solution is using an RGB-D camera or 3D LiDAR [22] or integrating a camera and 2D laser rangefinders [23] to get a complete environment representation. Nevertheless, this application can consume more power and reduce real-time performance during navigation tasks.

Lundell et al. [24] used a fully convolutional network (FCN) autoencoder to estimate laser rangefinder scanning with actual obstacle distances from 2D laser scans. Their later result [25] unified the processed laser scans into occupancy maps with uncertainty approximation. The actual obstacle distances data are collected for training with a 3D camera measurement. The authors presented that their strategy could avoid collisions with obstacles in real-world scenarios. This method depends on an additional RGB-D camera for making the training examples, which are discarded when implementing the navigation in realistic scenarios. Moreover, this method cannot be implemented directly in a different type of 2D LiDAR angle and range data.

Kollmitz et al. [14] proposed obstacle prediction networks for predicting unseen obstacle shapes in 2D map created with 2D laser rangefinders. Their strategy uses

a FCN trained from collision events recorded with a bumper. The results confirm that the trained FCN on a simulated collision dataset can predict and segment the unseen obstacles in a 2D map. They also demonstrate that the implementation of this method can be further enhanced by combining new obstacle examples collected during real-world applications.

The comparison result that indicates the advantages and limitations of obstacle prediction networks [14] with other various types of obstacle and local planners and sensor configuration has yet to be discussed in recent papers or in original papers. Therefore, we initiate to investigate the efficiency of this method and the conventional method for robot navigation in a 3D simulated environment. Since our robot has multiple sensors and cameras for manipulation and navigation, the combination sensor for the navigation task will spend more computation time. However, the computation cost is not our focus in this work. We focused on which method can enhance the robot's navigation efficiently and avoid collision in different types of objects that are difficult to detect by using laser rangefinders only. Using the Kollmitz et al. [14] result, we can rely on laser rangefinders only for navigation and decrease its limitation with the recent result of neural networks. We evaluated this result with RNS and various conventional local planners such as TEB Planner [18], DWA Planner [16], EBand Planner [17], and a global planner.

3. Method

In this section, we explain each step to investigate and evaluate the recent result of obstacle prediction networks and how to integrate it for local navigation in a 3D simulated world using Toyota HSR. First, we will explain how to obtain the predicted map using this method [14]. Afterward, the predicted map can be used for the RNS system for navigation tasks.

Robotic systems depend on accurate information about the environments they interact, particularly during navigation. In the previous works [9, 13, 21, 26], the recorded 2D map is used for DRL agents and the traditional local planner methods to learn or perform the local navigation, avoid dynamic and static obstacles, and find the best path to reach the goal. The recorded map (raw map), as shown in **Fig. 2**, generally can be obtained by using grid mapping [27], Hector SLAM [28] or Google Cartographer [29] to record the map from a real-world environment or 3D realistic simulation. First, we use the Kollmitz et al. trained architectures [14] to predict the unseen obstacle in our 2D recorded map that we collected from Hector SLAM by teleoperating the robot. The 2D map prediction is used to perform the navigation task. **Fig. 3** illustrates the process of how we obtained the predicted map by using Kollmitz et al. architectures. The authors use the LeNet architectures with a fully convolutional model to get shorter training process time and better accuracy. This model's dataset uses SceneNet [30], consisting of a 3D environment with 52 indoor scenes with

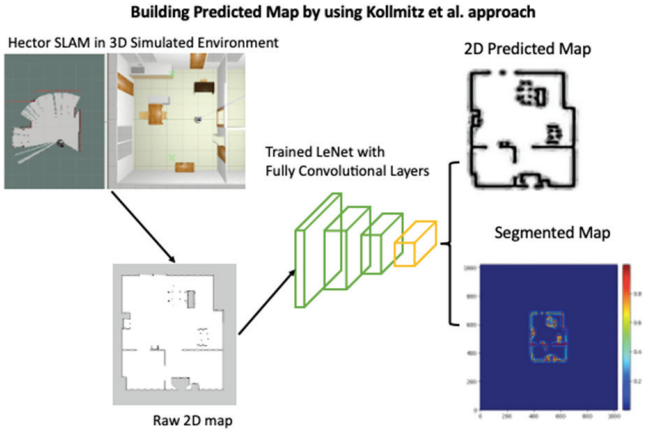

Fig. 3. Initial step to build the predicted map using this method [14].

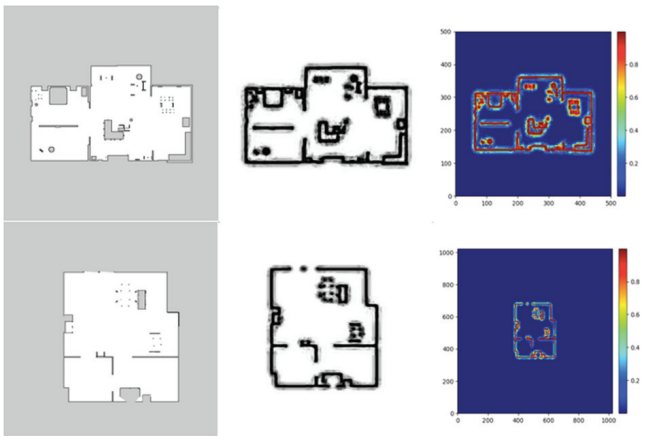

Fig. 4. Raw map, predicted map, and heat map from 3D environment of small house and large house.

various room layouts and furniture. The authors also used the simulated version of the service robot equipped with a sensitive force sensor that records the collision examples. The authors drove the robot to a random position in a simulated environment until they received the collision signal. Then collision data from the sensor are saved as the dataset. They divided the dataset into 34 rooms for training, 9 rooms for testing, and 9 rooms for validation.

To get the predicted 2D map, we inserted the raw maps that we obtained from Hector SLAM into a pre-trained neural network for collision prediction and segmentation. The segmentation result of a small house (SM) and large house (LH) can be seen in **Fig. 4**. The predicted map indicates the table legs and chair legs, and free space among them can be segmented as obstacle marks by using the trained networks in both maps. The heat maps result shows the data visualization representing the magnitude of a free-collision and collision area as colors in two dimensions. In **Fig. 4**, the raw map on the left side detects that the table and chair legs look like a tiny dot in the 2D occupancy map. On the other hand, the predicted map in the center visualized that the several small dots around

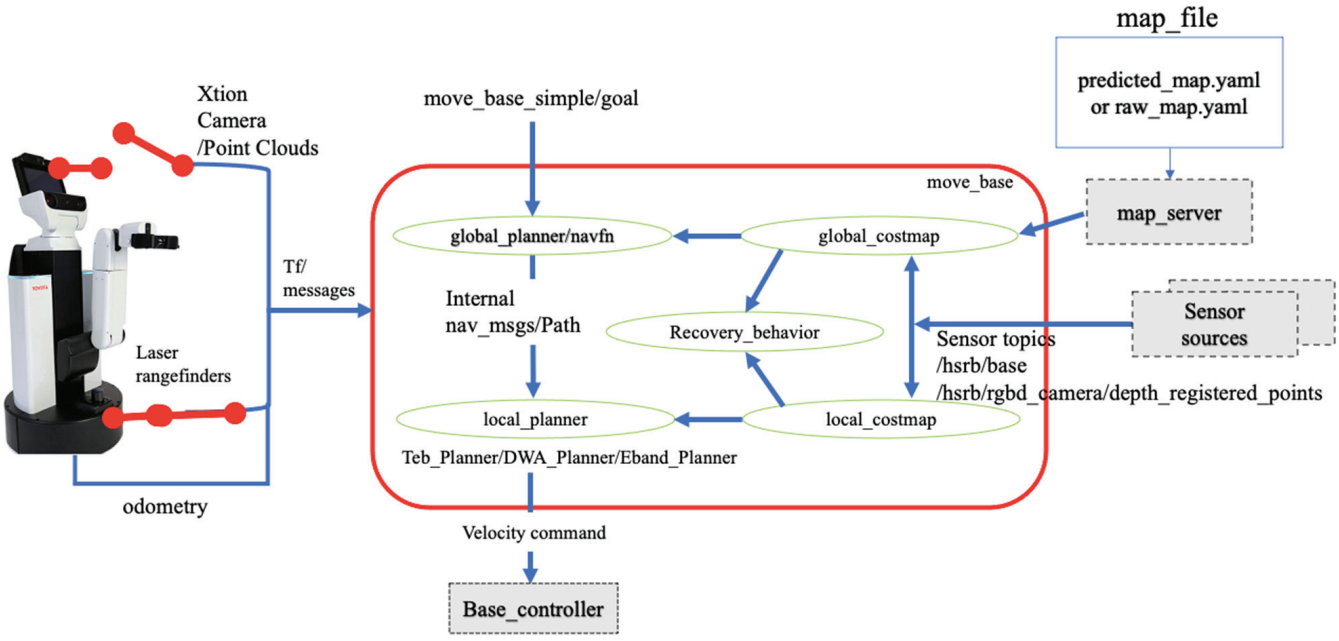

Fig. 5. General ROS navigation stack (RNS) design for investigating the effectiveness of predicted map based on sensor input from HSR sensor.

the table are merged, becoming a new obstacle footprint. For more explanation about the details of the network, architectures can be read in the original paper. To evaluate the effectiveness of the predicted map in local navigation, we designed the integration system based on RNS such as **Fig. 5**. A brief explanation of nodes from the integration system is as follows:

(i) *Global planner:* NavFn is a global planner node in RNS that drives on a 2D occupancy global costmap by using the Dijkstra strategy to achieve the goal point using the global map. This path message uses general type navigation msgs/Path.msg, which includes the waypoints without the orientation.

(ii) *Odometry:* In this system, we used wheel odometry which is used to create the ego-motion measurements from the starting point of the vehicle.

(iii) *Global and local costmap:* The local and global costmap nodes represent the robot of the vehicle to an obstacle using the robot geometry [31]. The 2D map has the obstacles inflated by a safety boundary where the robot is not allowed to enter. Moreover, this map is used by local and global planners to adjust the path based on the distance from the robot to the obstacles. We use the very small value of the inflated layer in each costmap to measure the effectiveness of the predicted map.

(iv) *Input/Sensor usage:* The integration of RGB-D camera and laser rangefinders with the raw map will be compared to laser rangefinders only with predicted maps. We also provide the experiment of the navigation with laser rangefinders only and with a raw map to know the robot is difficult to avoid the table, chair, and sports equipment such as in SH and LH 3D environments.

(v) *Transformation messages (tf):* tf message is a robot transform message in the ROS package which manages the position and orientation between various sensors connected to an HSR. In this case, the reference point of odometry is at the center of the robot base. So, a tf between the odometry (Odom), robot mobile base (base_link), and X-Tion camera and laser rangefinders is established using tf library in ROS.

(vi) *Recovery behavior:* This node provides the simple recovery motion to clear the space in the costmaps by rotating the robot 360°.

To get more detail explanation from ROS navigation stack, the detailed information is provided in this [15].

4. Experimental Setup

To test and evaluate the approach from [14], we formulate a simple test where the robot navigates from the initial point to several checkpoints and a final goal point. **Fig. 6** describes the robot navigation point in each environment. We designed the checkpoints based on the unseen obstacle position in the 3D environments to evaluate how the robot performance to avoid the unseen obstacle using different combinations of sensors, maps, and local planners.

The testing scenario is divided into 2 stages such as in **Table 1**. In each scenario, several combinations are configured in the RNS system and 3D environment to investigate and analyze the performance of robot naviga-

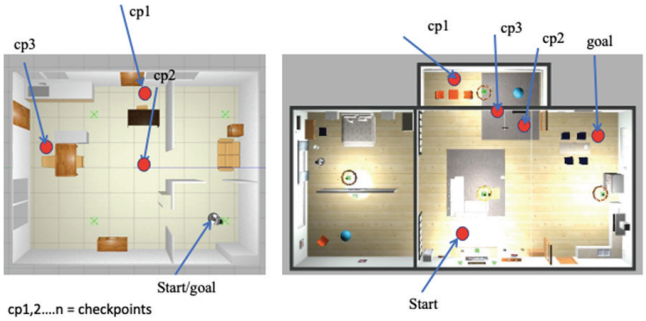

Fig. 6. Start, checkpoints, and goal for the robot navigation test in SH and LH.

Table 1. Stages of testing configuration.

	Global planner / NavFn		
	TEB Planner / DWA Planner / Eband Planner		
	Sensor	Map	Environment
Stage 1	Laser only	Raw	SH
	Laser + RGB-D	Raw	
	Laser only	Predicted map	
Stage 2	Laser only	Raw	LH
	Laser + RGB-D	Raw	
	Laser only	Predicted map	

tion with different types of unseen obstacles. The navigation parameters in RNS are defined in **Table 2**. We used small values on inflation radius to evaluate the effect of the 2D predicted map and 2D LiDAR only, navigation with sensor fusion and raw map, and raw map with 2D LiDAR only in the experiments. The inflation radius is a safety distance parameter around the obstacles. Suppose the value of the inflation radius is more than 0.1. In that case, the laser rangefinders can neglect the narrow free space between the table and chair legs. Also, sometimes robot is difficult to enter a narrow space.

We evaluate the efficiency of local planners with a different type of 2D map by calculating the path length and the average time to reach the goal. In addition, we define the percentage of the success rate of each episode based on achieved checkpoints (*cp*). If the robot cannot reach a *cp1* in less than 2 minutes, the navigation process to reach *cp1* will terminate and attempt to the next *cp*.

We used a laptop with Intel® Core TM i7-8750 CPU @ 2.20 GHz processors with eight cores, 16 GB RAM, NVIDIA GeForce RTX 2070 graphics card, and Ubuntu 18.04 LTS 64 bits operation system. The Toyota HSR is used for the development of this project [1]. It has an omnidirectional dual-wheel caster drive that can move in any direction on a 2D plane and sensors used for 2D and 3D cameras.

5. Results and Discussion

From 2 stages, 10 experiments were carried out for each local planner and map, environment, and sensor combination. 18 subsets of tests were conducted, totaling 180 navigation experiments in simulated environments. The primary purpose of these investigations is to evaluate the robot's navigation behavior in unseen obstacles, maps, and environments using 2D LiDAR only and sensor fusion. The raw map and laser rangefinders results indicate that the local planner could not generate a collision-free path when facing the table, chair, and sports equipment. On the other hand, the predicted map with 2D LiDAR only and sensor fusion with the raw map can still manage the difficult obstacle. In this experiment, we conduct different rules for this configuration. We terminate the simulation when the robot hits an obstacle or is freezing for more than a minute. It is difficult for the local planners to pass the table and chair safely by using raw map configuration as shown in **Fig. 7**. However, the trial-error parameter tuning in inflation layers can be used to find the appropriate inflation layer using the raw map and 2D LiDAR only. Nevertheless, this method is time-consuming and tedious because it was tried every time the map and environment change. **Table 3** presents the quantitative result from the navigation experiment. As we expected, all the local planners with laser and the 2D predicted map outperformed in each environment, and TEB Planner and EBand Planner managed a 100% success rate in SH and 75% in LH. In the predicted map, the local planners could find the

Table 2. Navigation parameters in RNS.

Costmap common parameters	
Parameters	Values
Radius	0.25
Laser_scan_layer:	
Topic:	hsrb/base_scan
Clearing	true
Obstacle_range	2.0
Raytrace_range	3.0
RGBD_layer:	
Topic:	/head_rgbd_sensor/ depth_registered_points
Clearing true	
Obstacle_range	6.0
Raytrace_range	10.0
Inflation radius	0.1
Cost scaling factor	10.0
Global costmap parameters	
Update frequency	10
Static map	true
Local costmap parameters	
Update frequency	10
Rolling window width	true
Height resolution	0.025
Publish frequency	1.0
Static map	false

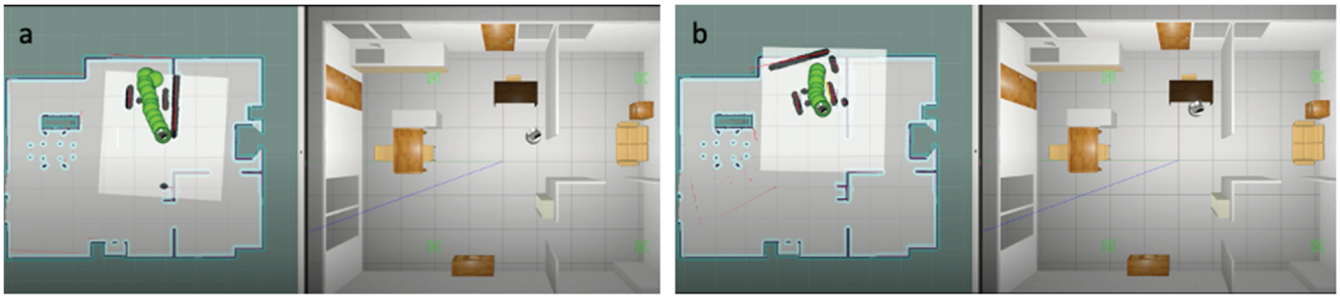

EbandPlanner with 2D raw map and SM

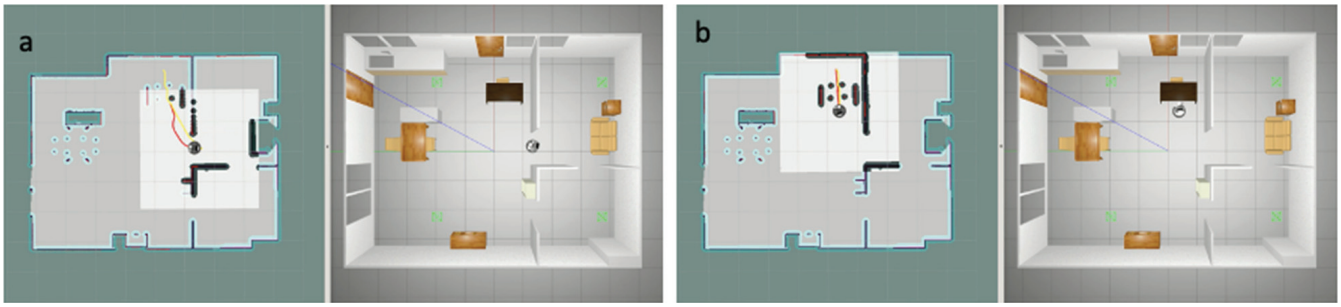

Tebplanner with 2D raw map and SM

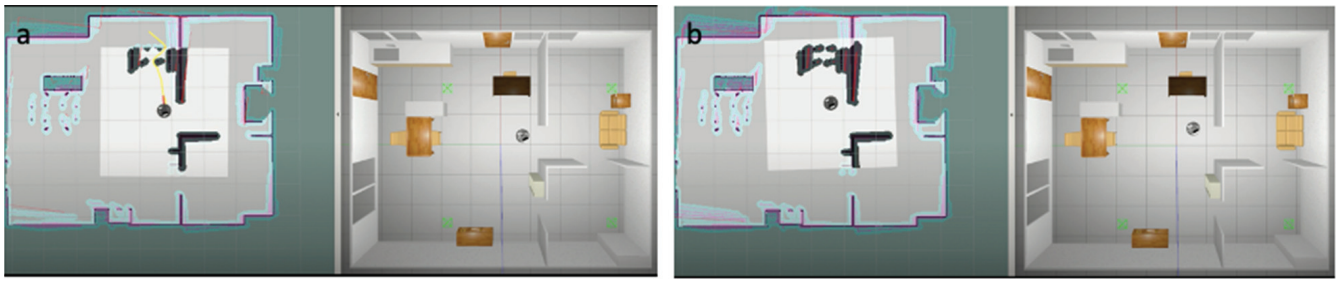

DWA with 2D raw map and SM

Fig. 7. Example results using the raw map and conventional local planners. The robot cannot avoid by only using laser rangefinders.

Table 3. Investigation and comparison result between 2D map prediction with RNS and conventional method.

	TEB+Laser				TEB+2Obs		DWA+Laser				DWA+2Obs		Eband+Laser				Eband+2Obs	
	Raw map		Predicted map		Raw map		Raw map		Predicted map		Raw map		Raw map		Predicted map		Raw map	
Evaluation	SH	LH	SH	LH	SH	LH	SH	LH	SH	LH	SH	LH	SH	LH	SH	LH	SH	LH
Average time [min]	1:00	1:00	2:41	4:21	2:39	4:34	1:00	1:00	3:41	4:16	4:01	4:20	1:00	1:00	3:11	4:52	3:10	4:57
Average path length [m]	8.7	7.9	36.5	24.4	36.4	25.36	8.7	7.9	31.5	25.21	19.44	25.23	8.7	7.9	36.8	25.33	21.34	25.56
Total success rate [%]	0	0	100	75	100	75	0	0	75	75	40	75	0	0	100	75	60	75

2Obs = RGB-D camera + 2D laser rangefinders

collision free path easily by only using the 2D LiDAR because the unseen obstacle has already been predicted by the obstacle prediction networks. When the robot faces the chair, table, and sports equipment, the tiny footprint represented in the raw map can be merged into the predicted map. Therefore, the free-collision area between tiny obstacles becomes new obstacle footprint that makes the local planner generate safer collision free path. The example behavior of the robot using the predicted map is shown in **Fig. 8**. DWA Planner with the predicted map only attains a 75% success rate in SH due to a freezing behavior when the robot approaches the *cp1* in SH but can safely avoid the obstacle in another unseen obstacle. It is due to the limitation of DWA Planner when facing the narrow space, as explained in [19]. All the local planners with a predicted map could not reach the maximum success rate in the LH environment. It is due to the mobile base colliding with the flat surface of the chair's leg, as shown in **Fig. 9**. This type of chair is hard for the robot to avoid collision by only using the laser rangefinders. Therefore, after the robot hits the chair, the robot will move to the following *cp* to finish the mission.

Figure 10 is an example of the robot avoiding collision with sports equipment objects using the laser rangefinders and RGB-D camera. When we used the conventional sensor fusion method, the detected free space between the

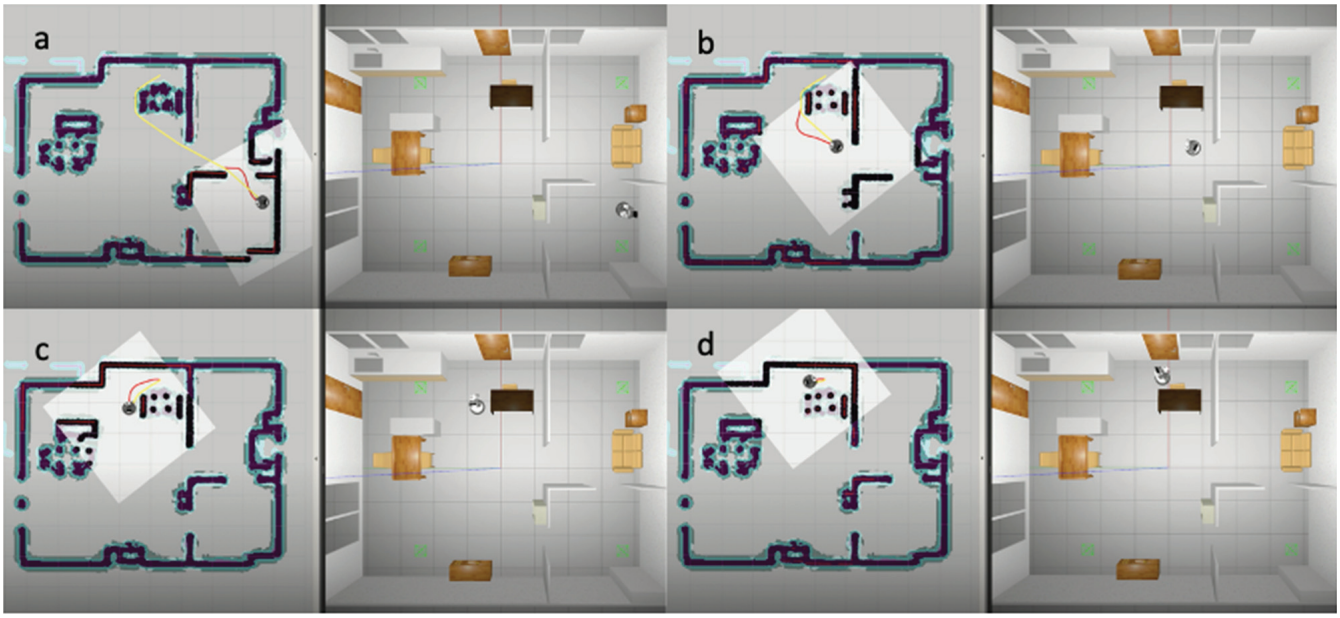

Fig. 8. The example results of using predicted map. We used laser rangefinders only. The predicted map has significant role to improve the navigation performance in real-world obstacle condition.

Fig. 9. The example results in failed navigation behavior using the predicted map and TEB Planners. The other planners also failed in this stage. The predicted map could not predict this type of chair. The leg part of the chair has a flat surface that is adhered to the floor.

wall and the table from the camera could be considered an alternative path for the robot. Nevertheless, the robot cannot pass the narrow space due to its size. Therefore, some local planners could not achieve the maximum success rate due to this limitation. TEB Planner achieves the best results among three conventional sensor fusion approaches with a success rate of 100% in SH and 75% in LH, while EBand Planner has second best performance and reached a success rate of 60% in SH and 75% in LH. DWA Planner has only reached a 40% success rate in SH and 75% in LH. Overall, the path length for each local planner with the highest success rate did not significantly differ. It is because we used only the static obstacle.

6. Conclusion

This paper presented an investigation and comparative study of the approach to solving unseen or partially observed obstacles using only laser rangefinders. We compare the result of Kollmitz et al. [14] with the conventional method to perform the navigation and avoid a collision from an object such as a table, chair, and sports equipment that are difficult for laser rangefinders to fully observe. The conventional method uses sensor fusion, such as a combination of RGB-D camera and 2D laser rangefinders. All methods were evaluated using the RNS in the simulated 3D environment. All the local planners with laser rangefinders and the 2D predicted map had achieved significant performance in each environment than only using the conventional method with raw map. Since the learning-based (DRL) local planner uses the

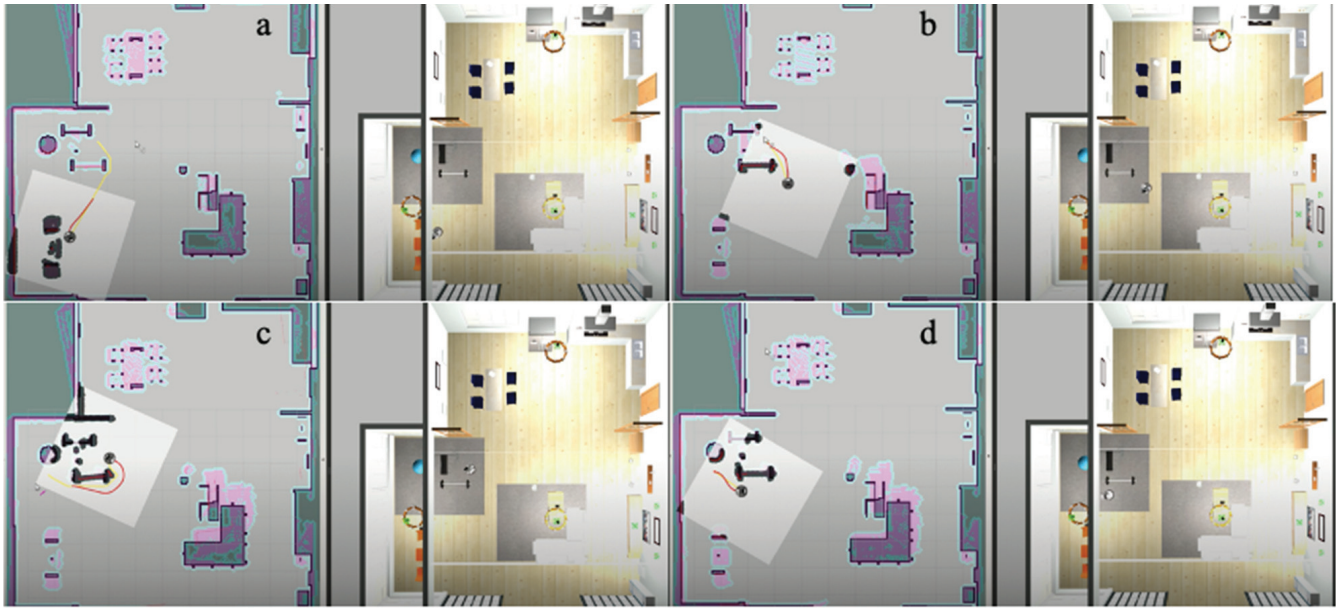

Fig. 10. The example results from using two observation resources. We used X-Tion RGB-D camera and laser rangefinders. The robot can avoid a collision with sports equipment obstacles.

recorded map to avoid static obstacles, the 2D predicted map could be considered a future work application for the learning-based local planner.

Acknowledgments

The authors would like to acknowledge the scholarship support provided by the Japan Ministry of Education, Culture, Sports, Science, and Technology (MEXT). This work was partially supported by Japan Science and Technology Agency (JST), Moonshot R&D, with grant number JPMJMS2034, and TMU local 5G research support.

References:

[1] T. Yamamoto, K. Terada, A. Ochiai, F. Saito, Y. Asahara, and K. Murase, "Development of the Research Platform of a Domestic Mobile Manipulator Utilized for International Competition and Field Test," IEEE Int. Conf. Intell. Robot. Syst., pp. 7675-7682, 2018. https://doi.org/10.1109/IROS.2018.8593798

[2] T. Yamamoto, K. Terada, A. Ochiai, F. Saito, Y. Asahara, and K. Murase, "Development of Human Support Robot as the research platform of a domestic mobile manipulator," ROBOMECH J., Vol.6, Article No.4, 2019. https://doi.org/10.1186/s40648-019-0132-3

[3] J. Kindle, F. Furrer, T. Novkovic, J. J. Chung, R. Siegwart, and J. Nieto, "Whole-Body Control of a Mobile Manipulator using End-to-End Reinforcement Learning," arXiv preprint, arXiv:2003.02637, 2020.

[4] J. Bohren et al., "Towards autonomous robotic butlers: Lessons learned with the PR2," Proc. IEEE Int. Conf. Robot. Autom., pp. 5568-5575, 2011. https://doi.org/10.1109/ICRA.2011.5980058

[5] F. Xia, C. Li, R. Martin-Martin, O. Litany, A. Toshev, and S. Savarese, "ReLMoGen: Integrating Motion Generation in Reinforcement Learning for Mobile Manipulation," 2021 IEEE Int. Conf. on Robotics and Automation (ICRA), pp. 4583-4590, 2021. https://doi.org/10.1109/icra48506.2021.9561315,

[6] M. Wise, M. Ferguson, D. King, E. Diehr, and D. Dymesich, "Fetch & Freight: Standard Platforms for Service Robot Applications," Work. Auton. Mob. Serv. Robot., held at 2016 Int. Jt. Conf. Artif. Intell., pp. 2-7, 2016.

[7] W. Garage, "PR2 User Manual," 2012.

[8] K. Blomqvist et al., "Go Fetch: Mobile Manipulation in Unstructured Environments," arXiv preprint, arXiv:2004.00899, 2020.

[9] R. Guldenring, M. Gorner, N. Hendrich, N. J. Jacobsen, and J. Zhang, "Learning local planners for human-aware navigation in indoor environments," IEEE Int. Conf. Intell. Robot. Syst., pp. 6053-6060, 2020. https://doi.org/10.1109/IROS45743.2020.9341783

[10] P. Singamaneni, A. Favier, and R. Alami, "Human-Aware Navigation Planner for Diverse Human-Robot Interaction Contexts," 2021 IEEE/RSJ Int. Conf. on Intelligent Robots and Systems (IROS), Prague, Czech Republic, pp. 5817-5824, 2021. https://doi.org/10.1109/IROS51168.2021.9636613

[11] P. Long, T. Fanl, X. Liao, W. Liu, H. Zhang, and J. Pan, "Towards optimally decentralized multi-robot collision avoidance via deep reinforcement learning," Proc. IEEE Int. Conf. Robot. Autom., pp. 6252-6259, 2018. https://doi.org/10.1109/ICRA.2018.8461113

[12] F. de A. M. Pimentel and P. T. Aquino-Jr., "Evaluation of ROS Navigation Stack for Social Navigation in Simulated Environments," J. Intell. Robot. Syst. Theory Appl., Vol.102, No.4, 2021. https://doi.org/10.1007/s10846-021-01424-z

[13] L. Kästner, T. Buiyan, X. Zhao, L. Jiao, Z. Shen, and J. Lambrecht, "Arena-Rosnav: Towards Deployment of Deep-Reinforcement-Learning-Based Obstacle Avoidance into Conventional Autonomous Navigation Systems," 2021 IEEE/RSJ Int. Conf. on Intelligent Robots and Systems (IROS 2021), 2021. https://doi.org/10.1109/iros51168.2021.9636226

[14] M. Kollmitz, D. Buscher, and W. Burgard, "Predicting Obstacle Footprints from 2D Occupancy Maps by Learning from Physical Interactions," Proc. IEEE Int. Conf. Robot. Autom., pp. 10256-10262, 2020. https://doi.org/10.1109/ICRA40945.2020.9197474

[15] E. Marder-Eppstein, E. Berger, T. Foote, B. Gerkey, and K. Konolige, "The office marathon: Robust navigation in an indoor office environment," Proc. IEEE Int. Conf. Robot. Autom., pp. 300-307, 2010. https://doi.org/10.1109/ROBOT.2010.5509725

[16] D. Fox, W. Burgard, and S. Thrun, "The Dynamic Window Approach to Collision Avoidance," IEEE Robot. Autom. Mag., Vol.4, No.1, pp. 23-33, 1997. https://doi.org/10.1109/100.580977

[17] S. Quinlan and O. Khatib, "Elastic bands: connecting path planning and control," 1993 IEEE Int. Conf. on Robotics and Automation, 1993. https://doi.org/10.1109/ROBOT.1993.291936

[18] C. Rösmann, F. Hoffmann, and T. Bertram, "Timed-Elastic-Bands for Time-Optimal Point-to-Point Nonlinear Model Predictive Control," 2015 European Control Conf. (ECC), pp. 3352-3357, 2015.

[19] U. Patel, N. K. S. Kumar, A. J. Sathyamoorthy, and D. Manocha, "DWA-RL: Dynamically Feasible Deep Reinforcement Learning Policy for Robot Navigation among Mobile Obstacles," 2021 IEEE Int. Conf. on Robotics and Automation (ICRA), Xi'an, China, pp. 6057-6063, 2021. https://doi.org/10.1109/ICRA48506.2021.9561462

[20] S. B. Banisetty, V. Rajamohan, F. Vega, and D. Feil-Seifer, "A deep learning approach to multi-context socially-aware navigation," 2021 30th IEEE Int. Conf. on Robot and Human Interactive Communication (RO-MAN 2021), pp. 23-30, 2021. https://doi.org/10.1109/RO-MAN50785.2021.9515424

[21] K. Li, Y. Xu, J. Wang, and M. Q. H. Meng, "SARL*: Deep reinforcement learning based human-aware navigation for mobile robot in indoor environments," IEEE Int. Conf. Robot. Biomimetics (ROBIO 2019), pp. 688-694, 2019. https://doi.org/10.1109/ROBIO49542.2019.8961764

[22] H. Darweesh et al., "Open source integrated planner for autonomous navigation in highly dynamic environments," J. Robot. Mechatron., Vol.29, No.4, pp. 668-684, 2017. https://doi.org/10.20965/jrm.2017.p0668

[23] K. Tobita, Y. Shikanai, and K. Mima, "Study on automatic operation of manual wheelchair prototype and basic experiments," J. Robot. Mechatron., Vol.33, No.1, pp. 69-77, 2021. https://doi.org/10.20965/jrm.2021.p0069

[24] J. Lundell, F. Verdoja, and V. Kyrki, "Hallucinating Robots: Inferring Obstacle Distances from Partial Laser Measurements," IEEE Int. Conf. Intell. Robot. Syst., pp. 4781-4787, 2018. https://doi.org/10.1109/IROS.2018.8594399

[25] F. Verdoja, J. Lundell, and V. Kyrki, "Deep network uncertainty maps for indoor navigation," IEEE-RAS Int. Conf. Humanoid Robot, Vol.2019-Oct., pp. 112-119, 2019. https://doi.org/10.1109/Humanoids43949.2019.9035016

[26] L. Kästner, T. Buiyan, X. Zhao, Z. Shen, C. Marx, and J. Lambrecht, "Connecting Deep-Reinforcement-Learning-based Obstacle Avoidance with Conventional Global Planners using Waypoint Generators," 2021 IEEE/RSJ Int. Conf. on Intelligent Robots and Systems (IROS 2021), 2021. https://doi.org/10.1109/iros51168.2021.9636039

[27] G. Grisetti, C. Stachniss, and W. Burgard, "Improved Techniques for Grid Mapping With Rao-Blackwellized Particle Filters," IEEE Trans. on Robotics, Vol.23, No.1, pp. 34-46, 2007. https://doi.org/10.1109/TRO.2006.889486

[28] S. Kohlbrecher, O. Von Stryk, J. Meyer, and U. Klingauf, "A Flexible and Scalable SLAM System with Full 3D Motion Estimation," IEEE Int. Symp. on Safety, Security, and Rescue Robotics (SSRR 2011), pp. 155-160, 2011.

[29] W. Hess, D. Kohler, H. Rapp, and D. Andor, "Real-time loop closure in 2D LIDAR SLAM," Proc. IEEE Int. Conf. on Robotics and Automation, Vol.2016-June, pp. 1271-1278, 2016. https://doi.org/10.1109/ICRA.2016.7487258

[30] A. Handa, V. Patraucean, S. Stent, and R. Cipolla, "Scenenet: An annotated model generator for indoor scene understanding," Proc. IEEE Int. Conf. Robot. Autom., Vol.2016-June, pp. 5737-5743, 2016. https://doi.org/10.1109/ICRA.2016.7487797

[31] D. V. Lu, D. Hershberger, and W. D. Smart, "Layered costmaps for context-sensitive navigation," IEEE Int. Conf. Intell. Robot. Syst., No.Iros, pp. 709-715, 2014. https://doi.org/10.1109/IROS.2014.6942636

Supporting Online Materials:

[a] J. Pages, L. Marchionni, and F. Ferro, "TIAGo: The Modular Robot That Adapts to Different Research Needs," Int. Workshop on Robot Modularity, pp. 3-6, 2016. https://clawar.org/wp-content/uploads/2016/10/P2.pdf [Accessed January 12, 2022]

[b] https://docs.hsr.io/hsrb_user_manual_en/index.html [Accessed January 17, 2022]

[c] https://aws.amazon.com/robomaker/ [Accessed January 17, 2022]

[d] S. Yao, G. Chen, Q. Qiu, J. Ma, X. Chen, and J. Ji, "Crowd-Aware Robot Navigation for Pedestrians with Multiple Collision Avoidance Strategies via Map-based Deep Reinforcement Learning." https://github.com/snape/RVO2 [Accessed January 21, 2022]

[e] B. P. Gerkey and K. Konolige, "Planning and Control in Unstructured Terrain," ICRA Work. Path Plan. Costmaps, 2008. http://pub1.willowgarage.com/apubdb_html/files_upload/8.pdf [Accessed January 21, 2022]

[f] B. Okal, T. Linder, D. Vasquez, S. Wehner, O. Islas, and L. Palmieri, "Pedestrian Simulator," 2018. https://github.com/srl-freiburg/pedsim_ros [Accessed January 30, 2022]

Name:
Mohamad Yani

ORCID:
0000-0001-5938-4430

Affiliation:
Lecturer, Department of Computer Engineering, Faculty of Electronics and Intelligent Industry Technology, Institut Teknologi Telkom Surabaya
Ph.D. Student, Department of Mechanical System Engineering, Faculty of System Design, Tokyo Metropolitan University

Address:
6-6 Asahigaoka, Hino, Tokyo 191-0065, Japan

Brief Biographical History:
2013 Received Bachelor of Applied Science in Electronic Engineering from Politeknik Elektronika Negeri Surabaya
2014- Firmware Engineer, Indonesia Epson Industry
2017 Received Master of Philosophy from Universiti Teknologi Malaysia (UTM)
2020 Graduated from Research Student Program, Tokyo Metropolitan University

Main Works:
• M. Yani, F. Ardilla, A. A. Saputra, and N. Kubota, "Gradient-Free Deep Q-Networks Reinforcement learning: Benchmark and Evaluation," 2021 IEEE Symposium Series on Computational Intelligence (SSCI), Orlando, FL, USA, pp. 1-5, 2021. https://doi.org/10.1109/SSCI50451.2021.9659941

Membership in Academic Societies:
• Institute of Electrical and Electronics Engineers (IEEE)

Name:
Azhar Aulia Saputra

Affiliation:
Assistant Professor, Department of Mechanical System Engineering, Faculty of System Design, Tokyo Metropolitan University

Address:
6-6 Asahigaoka, Hino, Tokyo 191-0065, Japan

Brief Biographical History:
2014 Received Bachelor of Applied Science from Politeknik Elektronika Negeri Surabaya
2018 Received Master of Engineering from Tokyo Metropolitan University
2019 Visiting Researcher, Ecole Polytechnique Federale de Lausanne (EPFL)
2021 Received Doctor of Philosophy from Tokyo Metropolitan University and received Excellent Graduate School Research Award from Japan Society of Automotive Engineers (JSAE)
2021- Postdoctoral Researcher, Department of Mechanical Systems Engineering, Graduate School of Systems Design, Tokyo Metropolitan University

Main Works:
• A. A. Saputra et al., "Topological based Environmental Reconstruction for Efficient Multi-Level Control of Robot Locomotion," 2022 Int. Electronics Symposium (IES), Surabaya, Indonesia, pp. 491-496, 2022. https://doi.org/10.1109/IES55876.2022.9888288

Membership in Academic Societies:
• Institute of Electrical and Electronics Engineers (IEEE)

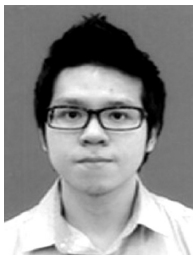

Name:
Wei Hong Chin

ORCID:
0000-0002-8592-9315

Affiliation:
Assistant, Department of Mechanical System Engineering, Faculty of System Design, Tokyo Metropolitan University

Address:
6-6 Asahigaoka, Hino, Tokyo 191-0065, Japan

Brief Biographical History:
2011 Received Bachelor's degree (Hons.) in Electronics Engineering, majoring in robotics and automation from Multimedia University
2015 Received Master's degree in Computer Science from University of Malaya
2019 Received Ph.D. from Tokyo Metropolitan University

Main Works:
• W. H. Chin, W. Dou, N. Kubota, and C. K. Loo, "A Robust Growing Memory Network for Lifelong Learning of Intelligent Agents," 2022 Int. Joint Conf. on Neural Networks (IJCNN), Padua, Italy, pp. 1-6, 2022. https://doi.org/10.1109/IJCNN55064.2022.9892827

Membership in Academic Societies:
• Institute of Electrical and Electronics Engineers (IEEE)

Name:
Naoyuki Kubota

ORCID:
0000-0001-8829-037X

Affiliation:
Department of Mechanical System Engineering, Faculty of System Design, Tokyo Metropolitan University

Address:
6-6 Asahigaoka, Hino, Tokyo 191-0065, Japan

Brief Biographical History:
1992 Received Bachelor's degree from Osaka Kyoiku University
1994 Received Master's degree from Hokkaido University
1997 Received Doctoral degree from Nagoya University
1997-2000 Assistant Professor and Lecturer in Mechanical Engineering, Osaka Institute of Technology
2000- Associate Professor, School of Engineering, Fukui University
2004-2012 Associate Professor, Graduate School of Engineering, Tokyo Metropolitan University
2012- Professor, Graduate School of Systems Design, Tokyo Metropolitan University

Main Works:
• N. Doteguchi and N. Kubota, "Topological Mapping for Event-based camera using Fast-GNG and SNN," 2022 IEEE Symposium Series on Computational Intelligence (SSCI), Singapore, pp. 984-989, 2022. https://doi.org/10.1109/SSCI51031.2022.10022102

Membership in Academic Societies:
• Institute of Electrical and Electronics Engineers (IEEE), Senior Member